Planar Squeeze Flow of a Bingham Fluid

Lorenzo Fusi[a], Angiolo Farina[a], Fabio Rosso[a]

[a]*Dipartimento di Matematica e Informatica "Ulisse Dini"*
Università degli Studi di Firenze
Viale Morgagni 67/a, 50134 Firenze, Italy

Abstract

In this paper we study the planar squeeze flow of a Bingham plastic in the lubrication approximation. We assume that the domain occupied by the fluid is closed at one end and open at the other (planar geometry). We consider two cases: *(i)* planar walls approaching each other in a prescribed way; *(ii)* parallel walls whose shape depends on both time and longitudinal coordinate. The dynamics of the unyielded region is determined exploiting the integral formulation of the linear momentum balance. We prove that in proximity of the closed end the material is always yielded, so that the rigid part is always detached from it. When dealing with case *(ii)*, we show that the dynamics of the rigid domain is governed by a very complex integral equation, whose qualitative analysis is beyond the aims of this paper. Conversely, in case *(i)* we obtain an almost explicit solution.

Keywords: Bingham fluid, Planar Squeezing, Lubrication Approximation

1. Introduction

A Bingham (or viscoplastic) fluid is a material that behaves as rigid body for low stress values, or as a viscous fluid (whose viscosity may depend on the local strain rate) when the stress state exceeds a critical threshold (we refer the readers to the original papers by Bingham [3], [4] or to [5]). As a consequence, unyielded regions that may stick to rigid walls or may be transported by the flow can develop within the material. In extreme cases, such regions may not exists at all or occupy the whole domain.

Modelling of Bingham materials has become increasingly important, especially because many materials encountered in industrial applications (e.g. foams, pastes, slurries, oils, ceramics, etc.) exhibit viscoplastic behaviour.

One of the most cited application of the Bingham model is toothpaste, which visually exhibits the fundamental character of viscoplasticity: it flows (i.e. deforms indefinitely) only if submitted to a stress above some critical value, otherwise it behaves as a solid body.

Despite the apparent simplicity of the constitutive models (especially when formulated within the implicit constitutive theory [17]–[22]) the flow characteristics of these materials are difficult to predict, since they involve unknown boundaries separating the yielded and the unyielded regions. This is noticeably evident when considering specific settings such as squeeze flow or channel flow with non uniform walls. In particular the squeeze problem has been the subject of a series of papers of both experimental and theoretical nature. Here we mention [8], [14], [16] [26],[20], [30] and the excellent paper [27], together with recent review by Coussot [7] and the numerous experimental papers therein cited.

When dealing with particular geometries that allow for major simplifications, such as the lubrication approximation [28], the Bingham model may lead to paradoxes or contradictions that invalidates the assumption of a perfectly rigid unyielded phase, [13]. This is the case, for instance, of the the well known "lubrication paradox", which essentially consists in the prediction of a plug speed that varies in the principal flow direction., meaning that a truly unyielded region cannot exist (see, for instance, [9], [15], [23] and [10]). This inconsistency has led some workers to consider strategies for overcoming the paradox. Balmforth and Craster [1] and subsequently Frigaard and Ryan [9] developed an asymptotic procedure that resolves the lubrication paradox and builds a consistent solution for thin layer problems In practice they resolve the paradox by considering higher order terms of the lubrication expansion and by showing that actually the plugs are slightly above the yield stress. They call these regions pseudo plugs and they prove that true rigid plugs are embedded within them.

In the case of a squeeze flow the problem is still not exhaustively studied, see [2]. For this peculiar problem the lubrication paradox was first pointed out by Lipscomb and Denn in [13], who simply proved that a central unyielded rigid core cannot exist because of symmetry reasons. A major analysis of the squeeze flow paradox between parallel discs was performed in [29], where the Bingham model was viewed as a limiting case of a bi-viscous fluid and where it was proved that the limiting process tending to the Bingham model and the lubrication approximation lead to a contradiction. In a recent paper by Muravleva [16] the planar squeeze flow of a Bingham fluid is stud-

ied exploiting the asymptotic technique introduced in [1]. This technique, which has been successfully exploited by Frigaard et al. [9] for the flow in a channel with slowly varying width, allows to determine intact true plug regions, overcoming thus the lubrication paradox.

In this paper we study the same problem presented in Muravleva [16], but we use a different approach developed in [10]. In this approach, which traces its roots back to [24] and [21], the whole unyielded region is treated as an evolving non material volume, whose motion is determined only by the stress applied by the fluid part. In practice the balance of linear momentum of the unyielded region is written using the integral form of the momentum balance, where only the external stress (i.e. the force exherted by the fluid) acting on the boundary is required.

The advantage of our procedure lies in the fact that no assumption has to be made on the order of magnitude of the stress components when applying the lubrication scaling. In our opinion this is the correct way to proceed, since in the rigid domain the Cauchy stress is "indeterminate" and we cannot identify or verify a posteriori which term can be safely neglected when applying the scaling. The main result we get is that we are able to determine a "true" unyielded plug and a "true" yielded surface directly at the leading order with a plug speed that does not vary in the principal flow direction (no pseudo-plug or fake yield surfaces). Moreover, differently from the vast majority of studies on squeeze flow of Bingham plastics, we do not suppose that the velocity of the plates is constant and that the gap width in which the fluid is confined does not vary with time.

We study the squeeze flow between parallel plates that are approaching each other in a prescribed way, i.e. planar squeeze flow. We begin by considering a planar geometry in which one end is closed, while on the other a known uniform pressure is applied[1]. Then, in Section 4, we consider the more general case of time-dependent non-flat walls. We develop the model assuming that the ratio ε between the maximum channel width and the channel length is very small, i.e. the lubrication regime. Accordingly the flow equations are drastically simplified and explicit solutions can be found.

We prove that the unyielded part is always detached from the closed end of the channel and confined between the squeezing surfaces. Actually

[1]We remark that assuming a "closed end" is equivalent to considering an open channel with symmetry condition.

the yield condition is met also at the channel closed end and in a portion of the mid-plane, but both regions have at least $O(\varepsilon)$ measure, so that the microscopic dynamics occurring there cannot be observed at the leading order approximation. Our analysis is indeed confined to the leading order and models the flow on a length scale where $O(\varepsilon)$ variations are not observable. A higher order analysis may lead to the detection of unyielded parts even in proximity of the above mentioned regions, as proved in [12].

2. Derivation of the model

Let us consider the flow of an incompressible Bingham fluid in a channel of length[2] L^* and amplitude $2h^*(t^*)$, as depicted in Fig. 1. Because of symmetry, we confine our analysis to the upper part of the layer, namely $[0, h^*(t^*)]$. The velocity field is $\mathbf{v}^* = u^*(x^*, y^*, t^*)\mathbf{i} + v^*(x^*, y^*, t^*)\mathbf{j}$, where x^*, y^* are the longitudinal and transversal coordinate respectively.

The Cauchy stress is $\mathbb{T}^* = -P^*\mathbb{I} + \mathbb{S}^*$, where $P^* = 1/3\mathrm{tr}\mathbb{T}^*$ and $\mathbb{S}$ is the so-called deviatoric part. The Bingham constitutive equation can be written in the implicit form [17]–[22]

$$\mathbb{D}^* = \left(\frac{II_{\mathbb{D}^*}}{2\eta^* II_{\mathbb{D}^*} + \tau_o^*}\right)\mathbb{S}^*, \tag{1}$$

which automatically gives the mechanical incompressibility condition $\mathrm{tr}\mathbb{D}^* = 0$. In particular η^* is the viscosity, τ_o^* is the yield stress and

$$\mathbb{D}^* = \frac{1}{2}\left(\nabla\mathbf{v}^* + \nabla\mathbf{v}^{*^{\mathrm{T}}}\right), \qquad II_{\mathbb{S}^*} = \sqrt{\frac{1}{2}\,\mathrm{tr}\;\mathbb{S}^{*2}}, \qquad II_{\mathbb{D}^*} = \sqrt{\frac{1}{2}\,\mathrm{tr}\;\mathbb{D}^{*2}}.$$

Equation (1) allows to express $\mathbb{S}^*$ as a function of $\mathbb{D}^*$ only when $II_{\mathbb{S}^*} \geq \tau_o^*$, while $\mathbb{D}^* = 0$, $\Leftrightarrow$ $II_{\mathbb{S}^*} \leq \tau_o^*$, the stress being constitutively indeterminate.

We assume that the region where $II_{\mathbb{S}^*} \geq \tau_o^*$ (yielded) and the region where $II_{\mathbb{S}^*} \leq \tau_o^*$ (unyielded) are separated by a sharp interface $y^* = \pm Y^*(x^*, t^*)$ called the "yield surface". We also define the inner plug

$$\Omega_{p^*}^* = \{(x^*, y^*) : \quad x^* \in [0, L^*], \quad y^* \in [-Y^*, Y^*]\}.$$

[2]The starred variables indicate dimensional quantities

Of course, it may occur that $Y^*(x^*,t^*)=0$ for some $x^*\in(0,L^*)$ and/or for some t^*, so that $\Omega^*_{p^*}$ becomes a segment of zero measure. The rigid plug $\Omega^*_{p^*}$ moves uniformly and its velocity is

$$\begin{cases} u^*=u^*_p(t^*), \\ \\ v^*=0, \quad \text{(by symmetry)}. \end{cases} \tag{2}$$

Considering a quasi-steady dynamics and neglecting body forces, the governing equations in the viscous region are the mechanical incompressibility condition

$$\mathrm{tr}\mathbb{D}^*=0,$$

and

$$-\frac{\partial P^*}{\partial x^*}+\frac{\partial S^*_{11}}{\partial x^*}+\frac{\partial S^*_{12}}{\partial y^*}=0, \tag{3}$$

$$-\frac{\partial P^*}{\partial y^*}+\frac{\partial S^*_{12}}{\partial x^*}+\frac{\partial S^*_{22}}{\partial y^*}=0, \tag{4}$$

where S^*_{ij} are the components of $\mathbb{S}^*$, given by (1), when $II_{\mathbb{S}^*}\geq\tau^*_o$.

The integral momentum balance for the whole domain $\Omega^*_{p^*}$, in the absence of body forces, is given by (see [11], [25] and [6])

$$\int_{\Omega^*_{p^*}}\frac{\partial}{\partial t^*}\left(\varrho^*\mathbf{v}^*\right)\mathrm{d}V^*+\int_{\partial\Omega^*_{p^*}}\varrho^*\mathbf{v}^*\left(\mathbf{v}^*\cdot\mathbf{n}\right)\mathrm{d}S^*=\int_{\partial\Omega^*_{p^*}}(\mathbb{T}^*\mathbf{n})\mathrm{d}S^*, \tag{5}$$

where ϱ^* is the material density. Neglecting the inertial terms, we get following equation[3]

$$\int_0^{L^*}\left[-Y^*_{x^*}T^*_{11}+T^*_{12}\right]_{Y^{*}+}\ \mathrm{d}x^*+P^*_{Y_0}Y^*_0-P^*_{Y_1}Y^*_1=0. \tag{6}$$

where $P^*_{Y_o}$, $P^*_{Y_1}$ represent the normal stresses on $x^*=0$ and $x^*=L^*$. Concerning the boundary conditions, we impose

$$\boldsymbol{v}^*\big|_{y^*=h^*}\cdot\mathbf{t}=0, \qquad \left(\mathbf{v}^*\big|_{y^*=h^*}-\mathbf{w}^*\right)\cdot\mathbf{n}=0, \tag{7}$$

[3]The expression $[-Y^*_x T^*_{11}+T^*_{12}]_{Y^*\,+}$ represents the force exerted by the viscous region on the lateral side of the inner rigid core.

$\mathbf{w}^* \cdot \mathbf{n}$ is the wall normal velocity and $\mathbf{t}$ is the wall tangent vector. On Y^* we write

$$[\![\mathbf{v}^*]\!]_{y^*=Y^*} = 0, \tag{8}$$

$$[\![\mathbb{T}^*\mathbf{n} \cdot \mathbf{t}]\!]_{y^*=Y^*} = 0, \qquad [\![\mathbb{T}^*\mathbf{n} \cdot \mathbf{n}]\!]_{y^*=Y^*} = 0, \tag{9}$$

while, on $x^* = 0$

$$\begin{cases} u^* = 0, \\ \\ S_{12}^* = 0, \end{cases} \tag{10}$$

In (8), (9) the symbol $[\![...]\!]$ denotes the jump across the interface $y^* = Y^*$ and we are also assuming $[\![\varrho^*]\!]_{y^*=Y^*} = 0$. Boundary conditions (10) are equal to the symmetry conditions one must impose on the symmetry axis when considering an open channel, as in [16].

3. Squeeze between parallel plates

We consider $h^* = h^*(t^*)$, and introduce

$$H^* = \max_{t^* \geq 0} h^*(t^*).$$

Next, we define the aspect ratio $\varepsilon = H^*/L^*$, assuming $\varepsilon \ll 1$. Then we rescale the problem using the following non dimensional variables

$$x = \frac{x^*}{L^*}, \qquad y = \frac{y^*}{\varepsilon L^*}, \qquad Y = \frac{Y^*}{\varepsilon L^*}, \qquad h = \frac{h^*}{H^*}, \qquad t = \frac{t^*}{T^*},$$

where T^* is the characteristic time scale, i.e. the "squeeze time". We define the characteristic transversal velocity as $V^* = H^*/T^*$, and the longitudinal velocity as $U^* = V^*/\varepsilon$, so that $u = u^*/U^*$, $v = v^*/V^* = v^*/(\varepsilon U^*)$. Concerning the pressure, exploiting the Poiseuille formula we define $P_c^* = (\eta^* L^* U^*)/{H^*}^2$ and set $P = P^*/P_c^*$, $P_{out} = P_{out}^*/P_c^*$, where P_{out}^* is the (given) pressure field applied at the channel outlet. We suppose that P_{out}^* is constant in time and space. Next we introduce

$$\mathbb{S} = \frac{\mathbb{S}^*}{(\eta_c^* U^*/H^*)}, \qquad \mathbb{D} = \frac{\mathbb{D}^*}{(U^*/H^*)}, \qquad II_{\mathbb{D}} = \frac{II_{\mathbb{D}^*}}{(U^*/H^*)}, \qquad II_{\mathbb{S}} = \frac{II_{\mathbb{S}^*}}{(\eta_c^* U^*/H^*)},$$

so that

$$\mathbb{D} = \frac{1}{2}\begin{bmatrix} 2\varepsilon\dfrac{\partial u}{\partial x} & \dfrac{\partial u}{\partial y} + \varepsilon^2\dfrac{\partial v}{\partial x} \\ \dfrac{\partial u}{\partial y} + \varepsilon^2\dfrac{\partial v}{\partial x} & 2\varepsilon\dfrac{\partial v}{\partial y} \end{bmatrix}, \qquad \mathbb{S} = \left(2 + \frac{\mathsf{Bi}}{II_D}\right)\mathbb{D},$$

where

$$\mathsf{Bi} = \frac{\tau_o^* H^*}{\eta^* U^*} \ = \frac{1}{\varepsilon}\frac{\tau_o^*}{P_c^*},$$

is the so-called Bingham number. The mechanical incompressibility constraint and momentum balance (3), (4) become

$$\frac{\partial u}{\partial x} + \frac{\partial v}{\partial y} = 0, \tag{11}$$

$$-\frac{\partial P}{\partial x} + \varepsilon\frac{\partial S_{11}}{\partial x} + \frac{\partial S_{12}}{\partial y} = 0, \tag{12}$$

$$-\frac{\partial P}{\partial y} + \varepsilon^2\frac{\partial S_{12}}{\partial x} + \varepsilon\frac{\partial S_{22}}{\partial y} = 0. \tag{13}$$

Equation (6) can be rewritten as

$$\int_0^1 \left[PY_x - \varepsilon Y_x S_{11} + S_{12}\right]_{Y^+} \, \mathrm{d}x + P_{Y_0}Y_0 - P_{out}Y_1 = 0, \tag{14}$$

where we have considered $P_{out} = P_{Y_1}$. Boundary conditions (7) become

$$u|_h = 0, \qquad v|_h = \dot{h}, \tag{15}$$

since the wall "squeeze velocity" (which is given) is $\dot{h} = \partial h/\partial t < 0$ (see [13]). Jump conditions (8) and (9) becomes

$$[\![u]\!]_{y=Y} = [\![v]\!]_{y=Y} = 0, \tag{16}$$

$$\begin{cases} [\![P]\!]\left[1 + \varepsilon^2\left(\dfrac{\partial Y}{\partial x}\right)^2\right]_{y=Y} + \left[\varepsilon^3 S_{11}\left(\dfrac{\partial Y}{\partial x}\right)^2 - 2\varepsilon^2 S_{12}\left(\dfrac{\partial Y}{\partial x}\right) + \varepsilon S_{22}\right]_{y=Y} = 0, \\ [\![S_{12}]\!]_{y=Y} + \varepsilon\left(\dfrac{\partial Y}{\partial x}\right)\left[S_{22} - S_{11} - \varepsilon S_{12}\dfrac{\partial Y}{\partial x}\right]_{y=Y} = 0, \end{cases} \tag{17}$$

while conditions (10) become

$$\begin{cases} u = 0, \\ \\ S_{12} = 0. \end{cases} \tag{18}$$

3.1. Model at the ε^0 approximation

Following [10], we look for a solution expressed as power series of ε, assuming $\mathsf{Bi} = \mathcal{O}(1)$. We remark that

$$S_{12} = \left[1 + \frac{\mathsf{Bi}}{|u_y|}\right] u_y,$$

becomes $S_{12}^{(0)} = u_y^{(0)} - \mathsf{Bi}$, since we are looking for a solution with $u_y^{(0)} < 0$ in the upper part of the channel. Thus equations (11)-(13) reduces to

$$\begin{cases} \dfrac{\partial u^{(0)}}{\partial x} + \dfrac{\partial v^{(0)}}{\partial y} = 0, \\ \\ -\dfrac{\partial P^{(0)}}{\partial x} + \dfrac{\partial}{\partial y}\left(\dfrac{\partial u^{(0)}}{\partial y}\right) = 0, \\ \\ -\dfrac{\partial P^{(0)}}{\partial y} = 0, \end{cases} \tag{19}$$

with boundary conditions

$$\begin{cases} \left.\dfrac{\partial u^{(0)}}{\partial y}\right|_{y=Y} = 0, \quad \Leftrightarrow \quad II_{\mathbb{D}}^{(0)} = 0, \quad \text{on} \quad y = Y, \\ \\ u^{(0)}(x, h, t) = 0, \quad \text{no} - \text{slip}. \end{cases} \tag{20}$$

To keep notation simple we suppress the superscript (0) and we denote $\frac{\partial f}{\partial t}$, $\frac{\partial f}{\partial x}$, $\frac{\partial^2 f}{\partial x^2}$ by f_t, f_x, f_{xx}, respectively. From $(19)_3$ we get $P = P(x, t)$, so that

$$u = -P_x \frac{(h - y)(y - 2Y + h)}{2}. \tag{21}$$

Exploiting $(19)_1$ along with (15), we find

$$\dot{h} - v\,(y, t) = \int_y^h \frac{\partial}{\partial x}\left[P_x \frac{(h - y')(y' - 2Y + h)}{2}\right] \mathrm{d}y' \ .$$

Next, evaluating u, v on Y and recalling conditions (16), we obtain

$$u|_{y=Y} = u_p(t) = -P_x \frac{(Y-h)^2}{2}, \tag{22}$$

$$v|_{y=Y} = \dot{h} + \frac{\partial}{\partial x}\left[P_x \frac{(Y-h)^3}{3}\right] - \frac{Y_x}{2} P_x (Y-h)^2 = 0. \tag{23}$$

The plug equation (14) becomes

$$\int_0^1 P Y_x \mathrm{d}x - \mathsf{Bi} + P_{Y_0} Y_0 - P_{out} Y_1 = 0,$$

or equivalently

$$-\int_0^1 P_x Y \mathrm{d}x = \mathsf{Bi}. \tag{24}$$

Recalling (18) we have $u_y = 0$ in $x = 0$ implying $P_x|_{x=0} = 0$. The solid region is then detached from $x = 0$, since otherwise $u_p \equiv 0$, i.e. no rigid domain motion. Accordingly there must be some $s\,(t) \in [0,1]$, not a priori known, such that $Y\,(x,t) \equiv 0$, for $0 \le x \le s\,(t)$. Hence the spatial domain $[0,1]$ can be split in two sub-domains (see Fig. 1):

- $0 \le x \le s\,(t)$, where $Y \equiv 0$;
- $s\,(t) < x \le 1$, where Y does not vanish.

Assuming that the longitudinal velocity is continuous across $s\,(t)$, we have

$$u_p(t) = -\frac{P_x\,(s,t)}{2}(\underbrace{Y\,(s,t)}_{0} - h)^2 = -\frac{P_x\,(s,t)}{2} h^2, \tag{25}$$

where $P_x\,(s,t)$ is unknown at this stage. From (23) we get

$$-\dot{h} + \frac{2}{3}\frac{\partial}{\partial x}\Big[-\underbrace{\frac{P_x}{2}(Y-h)^2}_{u_p(t)}\,(Y-h)\Big] - Y_x \underbrace{\left[-\frac{P_x}{2}(Y-h)^2\right]}_{u_p(t)} = 0,$$

namely

$$\dot{h} + \frac{1}{3} u_p(t) Y_x = 0, \tag{26}$$

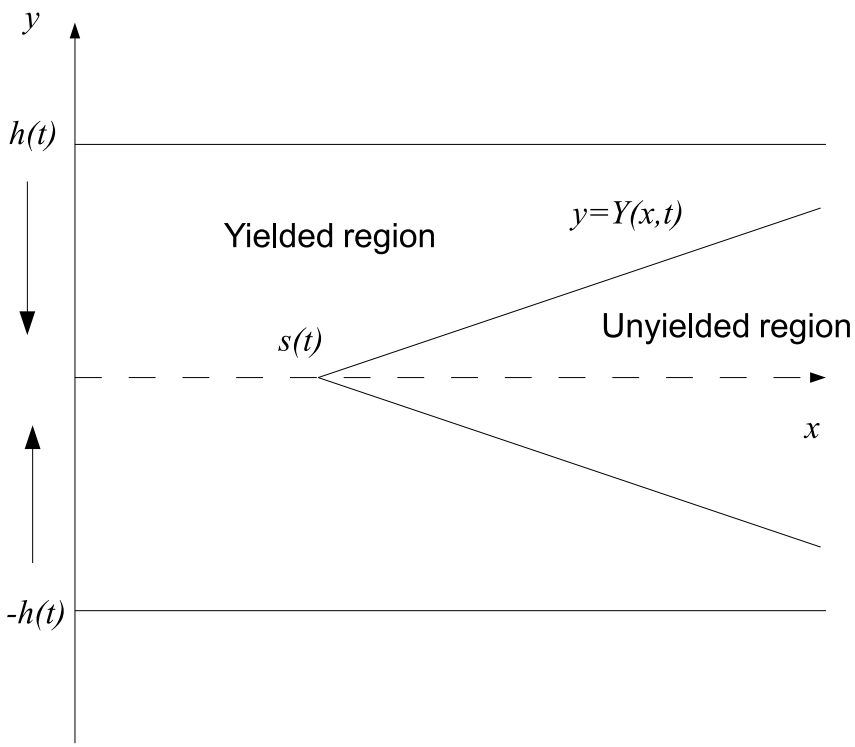

Figure 1: A schematic representation of the squeezing channel.

implying that Y is a linear non decreasing function of x. Thus, in order to avoid physical inconsistencies, we set

$$Y\left(x,t\right)=\max\left\{0,-\frac{3\dot{h}s(t)}{u_{p}(t)}\left(\frac{x}{s\left(t\right)}-1\right)\right\}. \tag{27}$$

The local instantaneous discharge is given by

$$Q\left(x,t\right)=\int_{0}^{Y}u_{p}\mathrm{d}y+\int_{Y}^{h}u\mathrm{d}y=u_{p}Y-\frac{P_{x}\left(x,t\right)}{3}\left(h-Y\right)^{3}. \tag{28}$$

Mass conservation then requires $Q\left(x,t\right)=-\dot{h}x$, so that $Q\left(s,t\right)=-\dot{h}s$, and

$$\underbrace{\frac{2}{3}\left(-\frac{P_{x}\left(s,t\right)}{2}h^{2}\right)}_{u_{p}(t)}h=-\dot{h}s,\quad\Rightarrow\quad u_{p}(t)=-\frac{3}{2}\frac{\dot{h}}{h}s, \tag{29}$$

which is positive since $\dot{h} < 0$. As a consequence

$$Y(x,t) = \max\left\{0,\ 2h(t)\left(\frac{x}{s(t)} - 1\right)\right\}. \tag{30}$$

The fluid squeezes out of the channel only if $Y(1,t) < h(t)$, namely when $s(t) > 2/3$. In $x \in [0,s]$ we have $Y = 0$ and the pressure fulfills equation (23) with the boundary condition $P_x(0,t) = 0$

$$\begin{cases} P_{xx} = \dfrac{3}{h^3}\dot{h}, \quad 0 < x < s, \quad t \geq 0 \\ \\ P_x(0,t) = 0 \quad t \geq 0. \end{cases}$$

Therefore

$$P(x,t) = \frac{3\dot{h}}{2h^3}x^2 + A(t),$$

with $A(t)$ still unknown at this stage. Recalling that Y is linear in x we integrate (22) between x and 1 getting

$$P(x,t) = P_{out} + \frac{3}{2}\dot{h}\left(\frac{s}{h}\right)^3\left[\frac{1}{2-3s} - \frac{1}{2x-3s}\right], \qquad s(t) < x \leq 1. \tag{31}$$

Then imposing the continuity of P across $x = s$ we get

$$P(x,t) = \frac{3\dot{h}}{2h^3}\left(x^2 - s^2\right) + P_{out} - 3\dot{h}\frac{s^2}{h^3}\left(\frac{s-1}{2-3s}\right), \qquad 0 \leq x \leq s(t). \tag{32}$$

Finally rewriting (24) as

$$\int_s^1 P_x Y \,\mathrm{d}x = -\mathsf{Bi},$$

we get

$$f(s) = s^2\left[\frac{2(1-s)}{3s-2} + \ln\left(\frac{3s-2}{s}\right)\right] = -\frac{2}{3}\frac{\mathsf{Bi}h^2}{\dot{h}}. \tag{33}$$

Hence, solving (33) we find $s(t)$ and we are able to determine the pressure field in the whole channel and the rigid domain as well. We observe that $s(t)$ is not a material point so that, in principle, $s(t)$ can also be still (i.e.

$\dot{s}(t) = 0$), while the rigid plug is moving with velocity $u_p(t)$. Fig. 2 shows the behavior of the function $f(s)$ in the l.h.s. of (33) with $s \in (2/3, 1)$. We easily realize that $f(s)$ is is monotonically decreasing for $2/3 < s \leq 1$ and that its range is $[0, +\infty)$. So, given any $-(2\mathsf{Bi}h^2)/(3\dot{h}) > 0$, there exists one and only one s fulfilling (33). From (31), (32) we compute the force acting

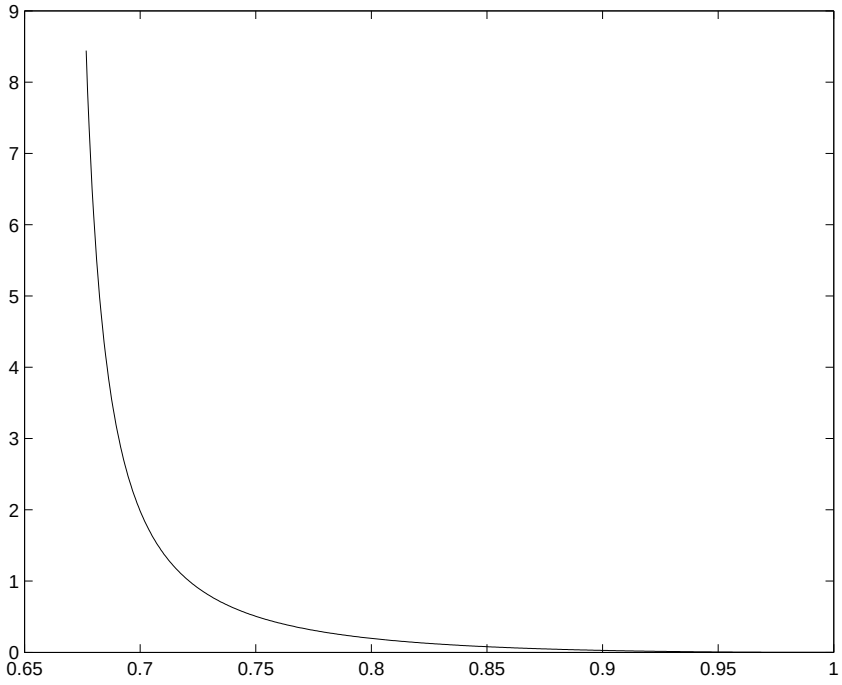

Figure 2: Behavior of $f(s)$ for $2/3 < s \leq 1$.

on the unit surface of upper plate, namely

$$P(t) = \int_0^1 P(x,t)\,\mathrm{d}x = P_{out} + \frac{\dot{h}s^3}{2h^3}\frac{5-3s}{2-3s} - \frac{3\dot{h}s^3}{4h^3}\ln\left(\frac{3s-2}{s}\right).$$

Exploiting (33) we get

$$P(t) - P_{out} = \frac{\mathsf{Bi}}{2}\frac{s}{h} - \dot{h}\left(\frac{s}{h}\right)^3\frac{1}{(3s-2)}. \tag{34}$$

Remark 1. We notice that in the domains

$$\mathcal{D}_1 = \{x = 0,\ 0 \leq y \leq 1\}, \qquad \mathcal{D}_2 = \{0 \leq x \leq s,\ y = 0\}. \tag{35}$$

the invariant $II_{\mathbb{D}} = 0$. This fact indicates that $\mathcal{D}_1$, $\mathcal{D}_2$ must be part of the unyielded portion of the fluid and, in principle, they should be embedded in the rigid plug. Actually this is not true since all the points lying in the vicinity of $\mathcal{D}_1$, $\mathcal{D}_2$ belong to the sheared part of the flow (yielded domain).

This "inconsistency" can be explained by observing that we can only state that $\mathcal{D}_1$, $\mathcal{D}_2$ are regions of zero measure at the zero order approximation, i.e. they appear to be 1D objects at the length scale that neglects $O(\varepsilon)$ terms. If we consider higher order expansions then we will likely find that $\mathcal{D}_1$, $\mathcal{D}_2$ are no longer 1D. This is exactly what happens in [12], [27], where an unyielded region of $\mathcal{O}(\varepsilon)$ thickness is found near $x = 0$.

In practice the "microscopic" dynamics occurring on $\mathcal{D}_1$, $\mathcal{D}_2$ cannot be observed macroscopically and we cannot rule out the existence of $\mathcal{O}(\varepsilon)$ unyielded regions in the vicinity of $x = 0$ and $y = 0$.

The same argument can be used to conclude that the linearity of Y in x holds only at the zero order. This would explain the discrepancies with some numerical simulations one can find in the literature that are performed for a "not so small" ε and that show nonlinear profiles of the yield surface (see [16]). Performing an asymptotic analysis that includes higher order terms, one could find a nonlinear correction of the yield surface profile which is clearly not "observable" at the leading order.

Remark 2. When $\mathsf{Bi} \to 0$, the solution of (33) is simply $s = 1$, i.e. the solid region does not exists at all (as physically expected for a Newtonian fluid). Furthermore formula (34) reduces to

$$P(t) - P_{out} = -\frac{\dot{h}}{h^3},$$

corresponding to the Newtonian fluid planar squeeze, [13]. These results confirms the physical consistency of our model.

3.2. Numerical simulation

In this section we perform some numerical simulations to analyse the behaviour of our asymptotic solution at the leading order. To illustrate the the dependence of the solution on the Bingham number we consider two

cases: $\mathsf{Bi} = 1$ and $\mathsf{Bi} = 25$. We plot the yield surface Y, the pressure field P and the axial velocity u, assuming that the plates have constant velocity so that

$$h(t) = 1 - t, \qquad \dot{h}(t) = -1. \tag{36}$$

This choice for $h(t)$ is completely arbitrary and can be obviously replaced with any other prescribed motion of the plates. We consider $t \in [0, 0.6]$, which guarantees that the plates do not come in touch in the select time interval. We set $h_f = h(0.6)$, representing the half gap width at time $t_f = 0.6$ and $s_f = s(0.6)$ representing the onset of the rigid plug at time $t = 0.6$. The yield surface Y and pressure field P are plotted for different times t belonging to the selected time interval and for $x \in [0, 1]$. The axial velocity u is plotted at time $t = 0.6$ (i.e. when $h = h_f$) for a finite number of $x \in [s_f, 1]$ and for y ranging in $[0, h_f]$.

In Fig. 3, 4 we have plotted the yield surface $Y(x, t)$ and the upper plate $y = h(t)$ at different times in the time interval $[0, t_f]$. We have plotted the upper plate only for $x \in [s(t), 1]$ so that the evolution of the onset of the plug $x = s(t)$ is visible. We notice that the slope of the unyielded plug becomes smaller as $s(t)$ increases, as expected. In Fig. 5, 6 we have plotted the pressure field at different times in the time interval $[0, t_f]$ in the whole domain $x \in [0, 1]$. Also for this case the position $x = s(t)$ has been put in evidence. We notice that the pressure within the gap increases as Bi increases.

In Fig. 7, 8 we have plot the axial velocity profile at time $t = 0.6$ for some fixed $x \in [s_f, 1]$. In particular velocity is plotted for $x = 0.69$, $x = 0.73$, $x = 0.77$, $x = 0.81$, $x = 0.85$. As one can easily observe the velocity of the plug is the same for each (x, y) belonging to the plug.
Finally in Fig. 9, 10 we have plotted the squeeze force given in (34) for different values of the Bingham number, Bi. We have plotted (34) for the linear squeeze (36) and for the exponential squeeze

$$h(t) = \exp(-t), \qquad \dot{h}(t) = -\exp(-t). \tag{37}$$

We observe that the linear squeeze requires a grater squeezing force than the exponential squeeze. This is physically consistent, since in the linear case the plates move faster than in the exponential case.

4. Squeeze between surfaces

In this section we generalize the problem to the case in which the parallel plates are surfaces $y = \pm h^*(x^*, t^*)$ that are approaching the channel

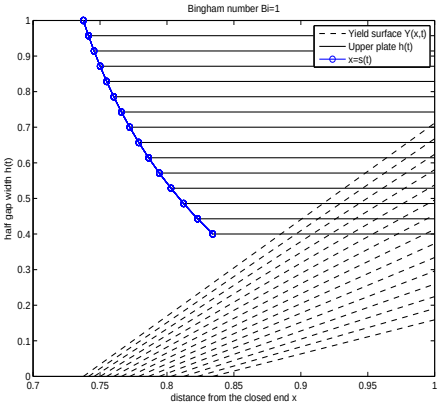

Figure 3: Y for $\mathsf{Bi} = 1$ and h given by (36)

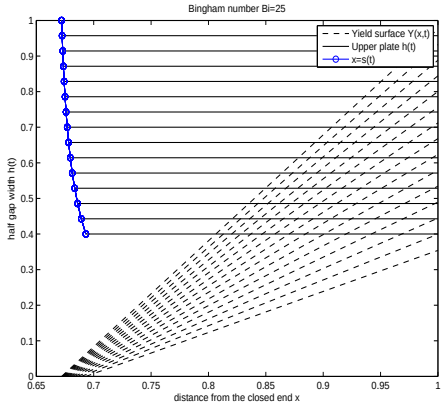

Figure 4: Y for $\mathsf{Bi} = 25$ and h given by (36)

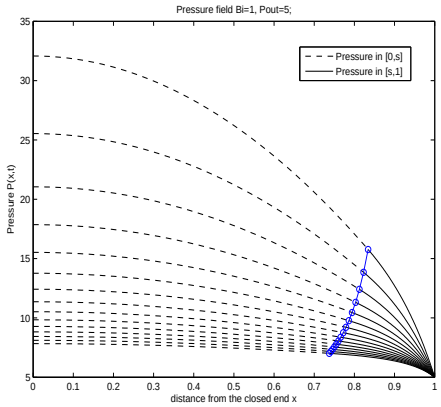

Figure 5: P for $\mathsf{Bi} = 1$ and h given by (36)

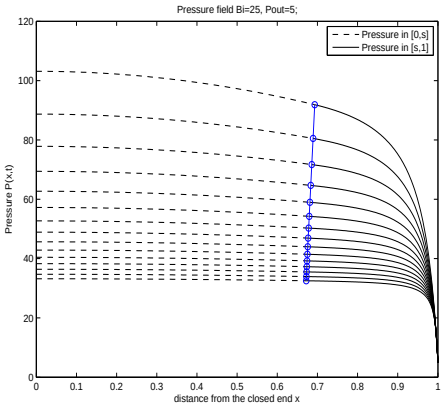

Figure 6: P for $\mathsf{Bi} = 25$ and h given by (36)

centerline, as shown in Fig. 11. In this case

$$H^* = \max_{\substack{x^* \in [0, L^*] \\ t^* > 0}} h^*(x^*, t^*),$$

and we again assume $H^*/L^* = \varepsilon \ll 1$. The theory develops exactly as in section 3, so that (24) still holds. We split $[0, 1]$ into $[0, s]$ and $[s, 1]$, so that continuity of u across $s\,(t)$ yields

$$u_p(t) = -\frac{P_x\,(s,t)}{2} h(s,t)^2.$$

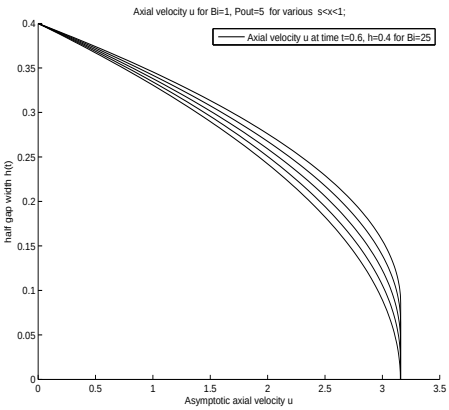

Figure 7: u for $\mathsf{Bi} = 1$ and h given by (36)

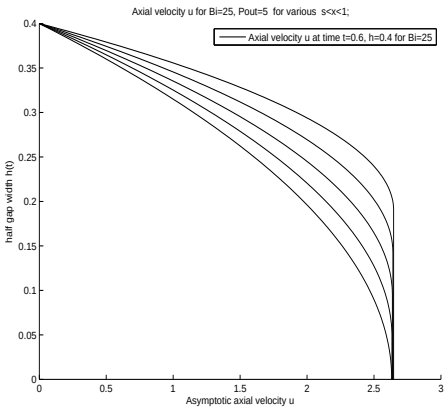

Figure 8: u for $\mathsf{Bi} = 25$ and h given by (36)

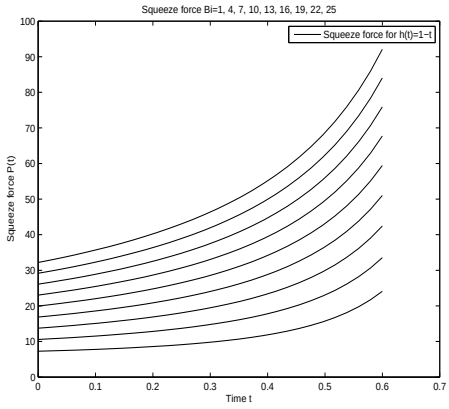

Figure 9: Squeeze force for linear $h(t)$, (36)

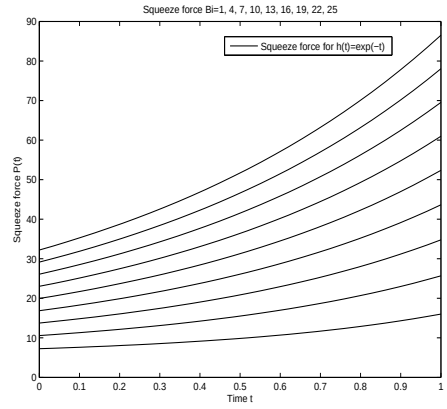

Figure 10: Squeeze force for exponential $h(t)$, (37)

Recalling (23) we find

$$h_t + \frac{1}{3}u_p(t)Y_x + \frac{2}{3}u_p(t)h_x = 0,$$

which generalizes (26). We thus get the following Cauchy problem

$$\begin{cases} Y_x = \dfrac{3}{u_p}\left[-h_t - \dfrac{2}{3}u_p h_x\right], \\ \\ Y(s,t) = 0, \end{cases}$$

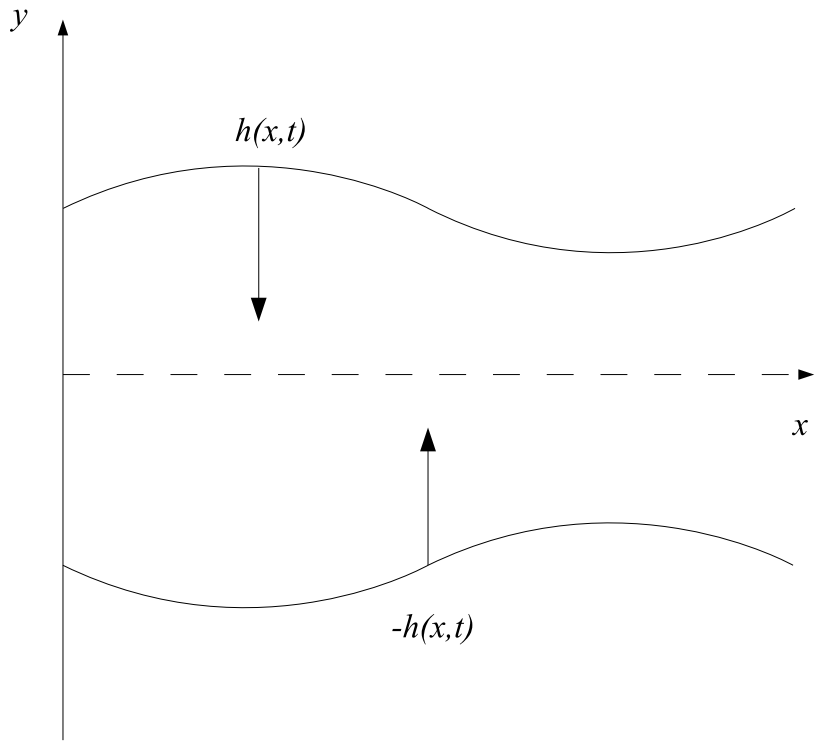

Figure 11: A schematic representation of the squeezing channel.

whose solution is

$$Y(x,t) = \frac{3}{u_p}\left[-\int_s^x h_t \mathrm{d}\xi - \frac{2}{3}u_p(h(x,t)-h(s,t))\right], \tag{38}$$

where s is still unknown. Following (27) we set

$$Y(x,t) = \max\left\{0,\ -\frac{3}{u_p}\int_s^x h_t \mathrm{d}\xi - 2(h(x,t)-h(s,t))\right\}. \tag{39}$$

The local discharge is

$$Q\,(x,t) = \underbrace{\int_0^Y u_p \mathrm{d}y}_{u_pY} + \underbrace{\int_Y^h \left[-P_x\frac{(h-y)(y-2Y+h)}{2}\right]\mathrm{d}y}_{-\frac{P_x(x,t)}{3}(h-Y)^3},$$

while mass conservation $h_t + Q_x = 0$ implies

$$Q(x,t) = -\int_0^x h_t \mathrm{d}\xi,$$

since $Q(0,t)=0$. We find

$$Q(s,t)=-\int_0^s h_t \mathrm{d}\xi=\underbrace{-\frac{P_x(s,t)h^2(s,t)}{2}}_{u_p}\frac{2h(s,t)}{3},$$

implying

$$u_p(t)=-\frac{3}{2}\frac{1}{h(s,t)}\int_0^s h_t \mathrm{d}\xi, \tag{40}$$

which is the generalization of (29). In conclusion, substituting (40) into (39), we find

$$Y(x,t)=\max\left\{0,\ -2h(x,t)+2h(s,t)\frac{\int_0^x h_t \mathrm{d}\xi}{\int_0^s h_t \mathrm{d}\xi}\right\}. \tag{41}$$

In $x\in[0,s]$ the pressure fulfils

$$\begin{cases} -h_t+\dfrac{\partial}{\partial x}\left[P_x\dfrac{h^3}{3}\right]=0, & 0<x<s\left(t\right), \\ & t\geq 0, \\ P_x\left(0,t\right)=0, & t\geq 0, \end{cases} \tag{42}$$

so that

$$P(x,t)=\int_0^x\left[\frac{3}{h(\tilde{x},t)^3}\int_0^{\tilde{x}} h_t \mathrm{d}\xi\right]\mathrm{d}\tilde{x}+A(t), \tag{43}$$

with $A\left(t\right)$ to be determined. In $x\in[s,1]$ we have

$$P_x(x,t)=-\frac{2u_p(t)}{(h-Y)^2},$$

so that

$$P_x=\frac{3}{h(s,t)\left[h(x,t)-Y(x,t)\right]^2}\int_0^s h_t \mathrm{d}\xi, \tag{44}$$

with Y given by (41). We observe that (42) and (44) yield $P_x|_{s^-}=P_x|_{s^+}$. Let us now integrate (44) between x and 1 with the boundary condition $P\left(1,t\right)=P_{out}$. We find

$$P_{out}-P\left(x,t\right)=\frac{3}{h(s,t)}\int_0^s h_t \mathrm{d}\xi\left[\int_x^1\frac{\mathrm{d}\ \tilde{x}}{\left(h(\tilde{x},t)-Y(\tilde{x},t)\right)^2}\right] \tag{45}$$

Imposing $P|_{s^-} = P|_{s^+}$, from (43), (45) we find $A(t)$, so that the pressure can be written in terms of s throughout the whole domain. Substituting (41) and (44) into (24) we get[4]

$$\int_s^1 \frac{\left[-2h(\tilde{x},t)+2h(s,t)\dfrac{\int_0^{\tilde{x}} h_t \mathrm{d}\xi}{\int_0^s h_t \mathrm{d}\xi}\right]_+}{\left[h(\tilde{x},t)-\left[-2h(\tilde{x},t)+2h(s,t)\dfrac{\int_0^{\tilde{x}} h_t \mathrm{d}\xi}{\int_0^s h_t \mathrm{d}\xi}\right]_+\right]^2}\mathrm{d}\tilde{x} = -\frac{\mathsf{Bi}}{\left[\dfrac{3}{h(s,t)}\int_0^s h_t \mathrm{d}\xi\right]}, \tag{46}$$

which provides an integral equation for the unknown $s(t)$. Equation (46) can be solved once we know the explicit form of the function $h(x,t)$.

When $h(x,t) = f(x)g(t)$, with[5] $f \cdot g > 0$, then (46) can be rewritten as

$$\left(\int_0^s f \mathrm{d}\xi\right)^2 \int_s^1 \frac{\left[-f(\tilde{x})\left(\int_0^s f \mathrm{d}\xi\right)+f(s)\left(\int_0^{\tilde{x}} f \mathrm{d}\xi\right)\right]_+ \mathrm{d}\tilde{x}}{\left[\dfrac{f(\tilde{x})}{2}\left(\int_0^s f \mathrm{d}\xi\right)-\left[-f(\tilde{x})\left(\int_0^s f \mathrm{d}\xi\right)+f(s)\left(\int_0^{\tilde{x}} f \mathrm{d}\xi\right)\right]_+\right]^2} =$$

$$= -\frac{2\mathsf{Bi} f(s) g(t)^2}{3\dot{g}(t)}. \tag{47}$$

Example 3. *Let us consider*

$$h(x,t) = f(x)g(t), \quad \text{with} \quad f(x) = \mathrm{e}^{-\beta x}, \quad g(t) = \mathrm{e}^{-\alpha t},$$

where α, and β both positive. Exploiting (47) we find

$$\frac{4(1-\mathrm{e}^{-\beta s})^2}{\beta}\int_s^1 \frac{(\mathrm{e}^{-\beta s}-\mathrm{e}^{-\beta x})}{[\mathrm{e}^{-\beta x}(3-\mathrm{e}^{-\beta s})-2\mathrm{e}^{-\beta s}]^2}\mathrm{d}x = \left(\frac{2\mathsf{Bi}}{3\alpha}\right)\mathrm{e}^{-\beta s}\mathrm{e}^{-\alpha t}. \tag{48}$$

[4]Notice that $\max\{0,\ f\} = [f\,]_+$, where $[f\,]_+$ denotes the positive part of f, i.e.

$$[f\,]_+ = \begin{cases} f, & \text{if} \quad f > 0, \\ 0, & \text{if} \quad f \le 0. \end{cases}$$

[5]f and g must have the same sign.

or equivalently

$$\underbrace{\frac{(1-\mathrm{e}^{-\beta s})^2}{\beta^2 \mathrm{e}^{-2\beta s}}\left[\ln\frac{|2+\mathrm{e}^{-\beta}-3\mathrm{e}^{\beta(s-1)}|}{|\mathrm{e}^{-\beta}-\mathrm{e}^{\beta(s-1)}|}+\frac{2(\mathrm{e}^{\beta(s-1)}-1)}{2+\mathrm{e}^{-\beta}-3\mathrm{e}^{\beta(s-1)}}\right]}_{\mathcal{G}(s)}=\left(\frac{2\mathsf{Bi}}{3\alpha}\right)\mathrm{e}^{-\alpha t}, \tag{49}$$

which is an implicit equation for $s(t)$. Notice that taking the limit $\beta \to 0$ of the l.h.s. of (49) we recover the l.h.s. of (33), as expected. The plot of $\mathcal{G}(s)$, for $\beta = 0.4$, is shown in Fig. 12. We immediately realize that (49) admits a

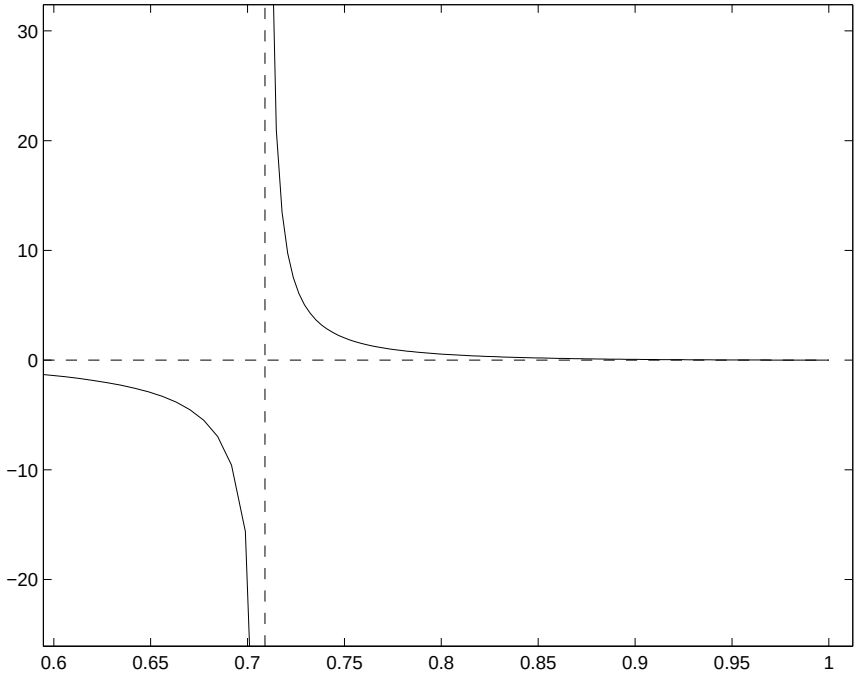

Figure 12: Behavior of $\mathcal{G}(s)$, with $\beta = 0.4$.

unique solution $s(t) \in (\hat{s}(\beta), 1]$, with

$$\hat{s}(\beta) = 1 + \frac{1}{\beta}\ln\left[\frac{\mathrm{e}^{-\beta}+2}{3}\right],$$

for each value of $(2\mathsf{Bi}/3\alpha)\,\mathrm{e}^{-\alpha t}$. *In particular it is easy to show that*

$$\frac{2}{3} < \hat{s}(\beta) < 1, \qquad \forall \beta > 0,$$

so that $s \in (2/3, 1)$ *for all* $t > 0$. *Recalling (41) we get*

$$Y(x,t) = 2\mathrm{e}^{-\alpha t}\left[\frac{\mathrm{e}^{-\beta s} - \mathrm{e}^{-\beta x}}{(1-\mathrm{e}^{-\beta s})}\right]. \tag{50}$$

Clearly $Y > 0$ *for every* $x > s$, *and* $Y = 0$ *at* $x = s$. *Actually we can show that* Y *and* h *never meets. Indeed, suppose that* $Y(x,t) < h(x,t)$, *then*

$$2\left[\frac{\mathrm{e}^{-\beta s} - \mathrm{e}^{-\beta x}}{(1-\mathrm{e}^{-\beta s})}\right] < \mathrm{e}^{-\beta x},$$

or analogously

$$2\mathrm{e}^{\beta x} < 3\mathrm{e}^{\beta s} - 1. \tag{51}$$

Hence $Y < h$ *if and only if (51) holds true for each* $x \geq s$. *Now recall that* $s \geq \hat{s}(\beta) > 2/3$, *for every finite time* $t > 0$ *and* $\beta > 0$. *Therefore*

$$2\mathrm{e}^{\beta x} \leq \max_{x\in[s,1]}\{2\mathrm{e}^{\beta x}\} = 2\mathrm{e}^{\beta} = 3\mathrm{e}^{\beta\hat{s}} - 1 < 3\mathrm{e}^{\beta s} - 1,$$

which proves that (51) holds true. As a consequence we get

$$0 \leq Y(x,t) < h(x,t), \quad \forall \;\; x \geq s, \quad t > 0.$$

We observe that $Y \to h$, *which in turn tends to* 0, *only in the limit* $t \to \infty$. *In Fig. 13 we have plot the advancing front* $x = s(t)$ *for different values of* Bi *ranging from* $\mathsf{Bi} = 0.1$ *to* $\mathsf{Bi} = 100$. *The parameters used are* $\alpha = 2$ *and* $\beta = 0.4$.

5. Conclusions

Many papers have been devoted to the squeeze flow between two coaxial flat disks. Here we do not consider the circular case, whose topology prevents the presence of any unyielded regions, but we focus on the simpler planar geometry, assuming further that the plates motion is prescribed. Operating in a lubrication framework, we model: *(i)* the flow caused by two

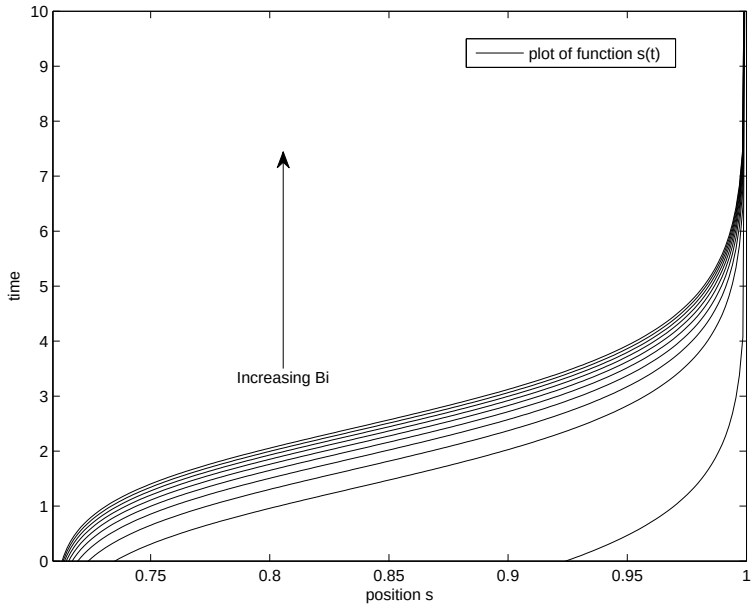

Figure 13: The advance of the front $x = s(t)$ for Bi ranging between 0.1 and 100.

parallel planes, of infinite width, that are approaching to one another; *(ii)* the squeeze caused by two symmetric surfaces (which may even change their shape over the time) approaching one to the other. In both cases we deal with a channel whose walls are symmetrically moving toward the centerline. In particular, one of the channel ends is closed while on the other an external known pressure is imposed.

Applying a technique developed in [10], which stems from the works by Safronchik [24] and Rubinstein [21], we have solved the flow in the yielded region and then modeled the unyielded dynamics simply exploiting the linear momentum balance for non material volumes. A simple physical argument led us to conclude that, at the leading order, any solid region has to be detached from the closed end of the channel. Hence a viscous region is located between $x = 0$, and $x = s\,(t)$, the latter being the abscissa of the incipient rigid region which extends from $y = -Y$ to $y = Y$. Actually, within the fully viscous region $II_{\mathbb{D}}$ vanishes in two domains of zero measure. This fact indicates the possibility that there may be unyielded areas of $\mathcal{O}\,(\varepsilon)$ measure, as shown in [12]. Actually, our two scale approach prevents a detailed analysis

of the dynamics at this scale (see Remark 1).

In section 4 we have generalized the problem considering plates whose shape may depend on x and t. We have proved that the evolution of the unyielded region is governed by a very complicated integral equation whose analysis is beyond the scope of the present paper. We have considered a special case in which the wall shape is the product of a function depending on time only and a function depending on space only (separation of variables). In this special case we have shown that the integral equation can be explicitly solved.

Acknowledgements

This work was supported by National Group of Mathematical Physics (GNFM - INdAM).

[1] Balmforth N.J., Craster R.V., A consistent thin-layer theory for Bingham fluids, J. Non-Newtonian Fluid Mech. **84** (1999) 65–81.

[2] Balmforth N.J., Frigaard I.A., Ovarlez G., Yielding to stress: recent developments in viscoplastic fluid mechanics, Annu. Rev. Fluid Mech. (2014) 121–146.

[3] Bingham E.C., An Investigation of the laws of plastic flow, U.S. Bureau of Standards Bulletin, **13** (1916) 309-353.

[4] Bingham E.C., Fluidity and plasticity, McGraw Hill (1922).

[5] Bird R.B., Stewart W.E., Lightfoot E.N., Transport phenomena, Wiley (1960).

[6] Coirier J., Mécanique des milieux continus, Dunod (1997).

[7] Coussot P., Yield stress fluid flows: a review of experimental data, J. Non-Newtonian Fluid Mech. **211** (2014) 31–49.

[8] Engmann J., Servais C., Burbidge A. S., Squeeze flow theory and applications to rheometry: A review, J. Non-Newtonian Fluid Mech. **132** (2005) 1–27.

[9] Frigaard I.A., Ryan D.P., Flow of a visco–plastic fluid in a channel of slowly varying width, J. Non-Newtonian Fluid Mech., **123**, (2004) 67–83.

[10] Fusi L., Farina A., Rosso F., Flow of a Bingham-like fluid in a finite channel of varying width: a two-scale approach, J. Non-Newtonian Fluid Mech., **177-178**, (2012), 76–88.

[11] Fusi L., Farina A., Rosso F., Roscani S., Pressure driven lubrication flow of a Bingham fluid in a channel: a novel approach, J. Non-Newt. Fluid Mech., **221** (2015), 66-75.

[12] Matsoukas A., Mitsoulis E., Geometry effects in squeeze flow of Bingham plastics, J. Non-Newtonian Fluid Mech., **109** (2003) 231–240.

[13] Lipscomb G.G., Denn M.M., Flow of Bingham fluids in complex geometries, J. Non-Newtonian Fluid Mech., **14** (1984) 337–346.

[14] Mitsoulis E., Flows of viscoplastic materials: Models and Computations, Rheology Reviews, (2007) 135-178.

[15] Putz A., Frigaard I.A., Martinez D.M., On the lubrication paradox and the use of regularisation methods for lubrication flows, J. Non-Newtonian Fluid Mech., **163** (2009) 62–77.

[16] Muravleva L., Squeeze plane flow of viscoplastic Bingham material, J. Non-Newt. Fluid Mech., **220** (2015) 148–161.

[17] Rajagopal K.R., On implicit constitutive theories, Appl. Math., **48**, (2003) 279–319.

[18] Rajagopal K.R., On implicit constitutive theories for fluids, J. Fluid Mech., **550**, (2006) 243–249.

[19] Rajagopal K.R., Srinivasa A.R., On the thermodynamics of fluids defined by implicit constitutive relations, ZAMP, **59** (2008) 715–729

[20] Ross A.B., Wilson S.K., Duffy B.R., Thin-film flow of a viscoplastic material round a large horizontal stationary or rotating cylinder, J. Fluid Mech., **430**, (2001), 309–333.

[21] Rubinstein L. I., The Stefan problem, Translations of Mathematical Monographs 27, American Mathematical Society, Providence R.I. (USA), (1971).

[22] Rajagopal K. R., Saccomandi G., Vergori L., Flow of fluids with pressure and shear-dependent viscosity down an inclined plane, J. Fluid Mech., **706** (2012) 173-189.

[23] Roussel N., Lanos C., Plastic fluid flow parameters identification using a simple squeezing test, Appl. Rheol. **13** (2003) 132-141

[24] Safroncik A. I., Nonstationary flow of a visco-plastic material between parallel walls, J. Appl. Math. Mech., **23**, (1959) 1314-1327.

[25] Serrin J., Mathematical principles of classical fluid mechanics, Handbuch der Physik, **8/1**, (1959) 125-263.

[26] Sherwood J.D., Durban D., Squeeze-flow of a Herschel-Bulkley fluid, J. Non-Newtonian Fluid Mech., **77** (1998) 115–121.

[27] Smyrnaios D.N., Tsamopoulos J.A., Squeeze flow of Bingham plastics, J. Non-Newtonian Fluid Mech., **100** (2001) 165–190.

[28] Stone H.A., On lubrication flows in geometries with zero local curvature, Chem. Eng. Sci., **60** (2005) 4838–4845.

[29] Wilson S.D.R., Squeezing flow of a Bingham material, J. Non-Newt. Fluid Mech., **47** (1993) 211–219.

[30] Wilson S.K., Duffy B.R., Ross A.B., On the gravity–driven draining of a rivulet of a viscoplastic material down a slowly varying substrate, Physics of Fluids, **14**, (2002) 555–571.